Numerical Prediction of Cavitation Inception in Centrifugal Impellers

NUMERICAL PREDICTION OF CAVITATION INCEPTION IN CENTRIFUGAL IMPELLERS

A. Marini[†] *- S. Salvadori*[†] *- C. Bernardini*[†] *- M. Insinna*[†]
F. Martelli[†] *- A. Nicchio*[‡] *- A. Piva*[‡]

[†]Energy Engineering Dept., University of Firenze, Italy
[‡]WEIR Gabbioneta srl, Milano, Italy

ABSTRACT

Cavitation is a fundamental issue in pump design since it yields significant decrease of performances and pump life, damaging impeller surfaces and triggering harmful flow instabilities. This topic is usually addressed through costly experimental tests. The aim of this paper is to assess numerical methodologies for the correct evaluation and prediction of the cavitation inception in centrifugal impellers during the design phase. Preliminary analyses were performed to individuate the most promising approach by using two cavitation models on a 2D test case representing the NACA 0009 hydrofoil. Then, two CFD approaches were considered for the evaluation of the NPSHr in actual pumps. RANS two-phase calculations including the selected cavitation model were performed on a geometry provided by WEIR Gabbioneta srl. Monophase simulations have been performed as well and an in-house heuristic model has been proposed to evaluate the NPSHr curve from a non cavitating pressure field. The heuristic post-processor has been tuned using both the two-phase and the monophase data, and validated using the available experimental values provided by WEIR Gabbioneta srl.

NOMENCLATURE

BEP	[-]	best efficiency point
l	$[m]$	turbulence length scale
H	$[m]$	head
$NPSHr$	$[m]$	required net positive suction head
n_s	$[m^{3/4}/s^{3/2}]$	specific speed
p_{ref}	$[Pa]$	reference pressure
p_{sat}	$[Pa]$	saturation pressure
Q	$[m^3/s]$	flow rate
Tu	$[\%]$	turbulence intensity
U_{ref}	$[m/s]$	reference velocity
y^+	[-]	dimensionless wall distance
ρ_l	$[kg/m^3]$	liquid phase density
ω	$[s^{-1}]$	specific turbulence kinetic energy dissipation

INTRODUCTION

Cavitation is a paramount issue for pump designers. Its development is responsible for noise production and damage of the impeller surfaces. Under certain working conditions, fluid pressure decreases under the saturation value and bubbles appear. Due to the density step between the two phases, steam volume is much higher than the corresponding water volume. Bubbles move toward the exit section driven by the positive pressure gradient. Then, implosion occurs and the surfaces are continuously subject to tough forces. This phenomenon is called ”pitting” and is responsible for pump mechanical deterioration. Also the pump performances are affected by cavitation insurgence, since both head and efficiency decrease when bubbles appear.

Even though the change of phase is always correlated to the pressure decrease, cavitation appears in several sections with many modalities. A classification has been proposed by Brennen (1994). Considering an unshrouded axial pump, the tip leakage vortex development generates low pressure zones near the top end-wall and the *tip vortex cavitation* (*TVC*) can occur near the blade leading edge. When considering an unshrouded impeller operating at a very low mass-flow rate, the tip leakage vortex can move upstream of the inlet section. If *TVC* occurs, the bubbles could recirculate across the inlet section as well. In this case the phenomenon is called *backflow cavitation*.

In an axial or centrifugal pump the water pressure level could reach the saturation value before the blade section. Then, bubbles appear before the inlet plane and *bubble cavitation* occurs. The most common cavitation insurgence is related to the flow acceleration on the blade suction side. This case is called *blade cavitation* and can be divided into two sub-categories. When bubbles collapse on the suction side surface a *partial cavitation* occurs. This is the most dangerous case due to the pitting occurrence. When bubbles are transported downstream of the blade trailing edge and collapse in the region before the volute *supercavitation* occurs. The main advantage of the latter case is that the pitting is neglected as well as the surface damage.

For all these reasons, predicting cavitation is a key aspect of pump design. This topic is usually focused through costly experimental tests. Nowadays, the available computational resources allow evaluating cavitation also using numerical models implemented in state-of-the-art Computational Fluid Dynamics (CFD) codes. According to the classification proposed by Tamura and Matsumoto (2009), the numerical approaches can be divided into two main groups: the interface tracking methods, like Volume of Fluid (VOF) methods (Kunz *et al*. (1999)), and the continuum modelisation, like the Barotropic (BT) methods (Delannoy and Kueny (1990)) and the Bubble Dynamics (BD) methods (Singhal *et al*. (2001), Schnerr and Sauer (2001), Zwart *et al*. (2004)).

A brief description of the methods follows. The VOF method is used when a large portion of the fluid is going to cavitate, e.g. in case of *blade cavitation*. Barotropic methods are able to resolve cases with small cavitating bubbles (e.g. *TVC* and *backflow cavitation*). A barotropic law is chosen to link steam/water density to the local pressure value. The slope of the curve between the two phases is defined as a function of the minimum sound speed in the mixture.

With the bubble dynamics method both accumulation and collapse of the bubbles can be considered. For this reason these methods can be used in a wide range of cases, except for cases with very large void fractions. In fact, the main drawback of the BD methods is that bubble-bubble interactions are negligible and a large steam portion generates numerical instability.

Amongst the BD methods, the algorithms proposed by Singhal *et al*. (2001), Schnerr and Sauer (2001) and Zwart *et al*. (2004) are the most interesting. A detailed description of the methods can be found in the cited papers while the main characteristics are listed below. All these methods use the same steam transport equation and the same bubble dynamics considerations. These methods differ by the definition of the vapor volume fraction α and of the net phase change rate R. The key parameter for those methods is represented by the bubble number density n, that represents the number of bubbles per unit volume. Through this number it is possible to evaluate the α parameter via the bubble radius value. With this approach the evaluation of R can be performed numerically once the local values of density, pressure, α and bubble radius are available.

Nowadays, the application of the cited methods to real centrifugal pumps seems to be limited to high level research performed by industrial labs or research centres. The only explanation is that up to now the necessary computational resources were not easily available. In fact, a good estimation of the required Net Positive Suction Head (NPSHr) can be obtained only using computational meshes with well discretized blade surfaces and CFD codes able to resolve unsteady cavitation (at least using a frozen rotor approach). For these reasons, the authors decided to evaluate the reliability of cavitation models when studying an in-line centrifugal pump. The numerical campaign have been realized

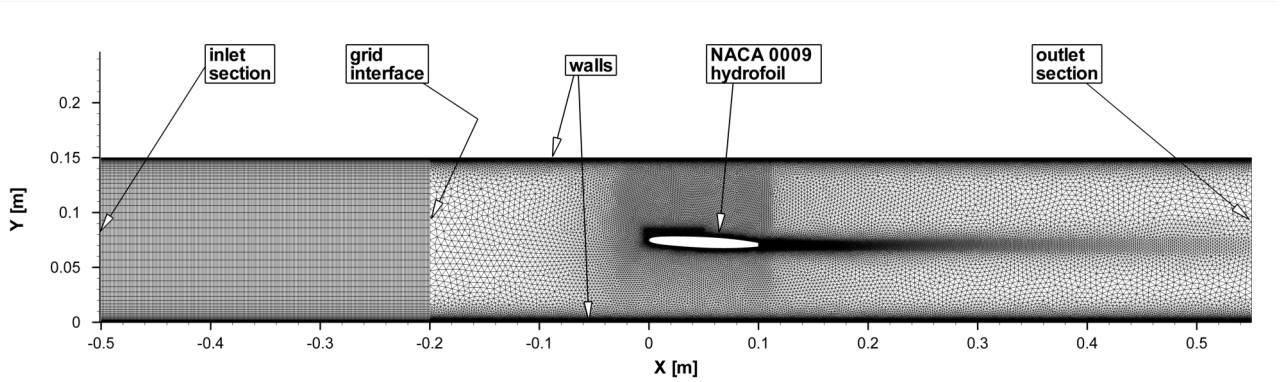

Figure 1: **Test case's grid composed by a structured zone and an hybrid unstructured zone**

using the ANSYS Fluent CFD code. In the present study the bubble dynamics methods have been considered due to their wide range of applications. Experimental data, as well as pump geometry, has been prepared by WEIR Gabbioneta.

From an industrial point of view, a more interesting approach would be to evaluate cavitation from a single phase CFD analysis. Therefore, correlations between the working conditions, the estimated pressure field of the pump and the NPSHr value have been investigated.

The paper is divided into three main sections. In the first part the Schnerr-Sauer and the Zwart methods are used to evaluate the pressure coefficient over a NACA 0009 profile in cavitating conditions. Based on the obtained results, the most promising model is used for the evaluation of the NPSHr of a centrifugal pump using two-phase simulations (in the second part of the paper). Comments on the development of an heuristic model for the NPSHr evaluation from single-phase calculations are presented in the final part.

VALIDATION OF THE NUMERICAL MODELS

The aim of this part of the work is to analyze, in terms of accuracy and numerical stability, some cavitation models implemented in the ANSYS Fluent commercial code on a 2D test case. The most promising approach will be used to study the cavitation on a complex case represented by an in-line centrifugal pump typical of oil & gas applications. The goal is to use a commercial CFD code for accurate prediction of the machine performance under cavitating conditions.

The selected test case is the NACA 0009 hydrofoil mounted into a square-section channel and invested by a water flow, both in non-cavitating and cavitating conditions. The profile is characterized by a maximum thickness of 10 mm and is truncated for mechanical reasons at 90% of the chord. Experimental data from Dupont (1991) were used to validate the numerical results. The experiments were simulated in Fluent using a computational domain that reproduces the test section of the water tunnel.

Numerical approach

The grid used for the simulations is shown in Figure 1. It is composed by two zones: a first one, structured, adjacent to the inlet section and a second one, hybrid unstructured, in which the NACA 0009 profile is located, with an angle of attack of 2.5 degrees. The structured grid was realized using an in-house tool while the test section is modeled using the commercial grid generator Centaur. The zones are joined by a grid interface. Special attention was posed in the dimension of the elements facing with each other in the boundary layer and the free stream zones.

The extension of the domain upstream of the profile has been created to allow the boundary layer development on the end-walls before the leading edge of the hydrofoil. It has been observed that without the extension, the free stream velocity was different from the experimental one and caused a wrong angle of attack of the flow. This approximation influences the pressure distribution along the hydrofoil, especially in cavitating conditions.

Particular attention was posed in the discretization of the leading edge and of the suction side. In fact, their influence on the bubble development is crucial and a local refinement was realized. Along the profile ten prismatic layers were posed and the width of the first layer was chosen in order to obtain $y^+ \leq 1$. The whole grid is composed by about 300k elements.

The full set of Reynolds-averaged Navier-Stokes equations were solved with the assumptions of a steady flow. The effects of turbulence were considered using the SST model by Menter (1992). This model allows resolving with high accuracy the near-wall region. The SIMPLE scheme was used for pressure-velocity coupling, a second-order up-wind scheme was considered for the momentum equations and the first-order up-wind scheme for the turbulence and vapor transport equations. Convergence was monitored taking into account the residuals, the mass balance and the pressure value on the blade surface. The calculations were considered to be converged once all the parameters were constantly lower than a specified value and almost constant over the numerical iterations.

For the cavitation modeling the Schnerr-Sauer (Schnerr and Sauer (2001)) and the Zwart-Gerber-Belamri (Zwart *et al*. (2004)) models were considered. The model of Singhal *et al*. (2001) is also implemented in Fluent, but is was discarded due to previously encountered stability problems. The Schnerr-Sauer model is the most promising one, since it has already been successfully used for an airfoil and a radial pump by Frobenius *et al*. (2003). It must be considered that in that case the model was implemented by Frobenius in their in-house code NS3D, developed at the Munich University of Technology. In cavitating conditions, slip velocity between cavitation bubbles and liquid was not taken into account. The authors think that in this test case the domain is not subject to any acceleration field, whereby the density difference between vapor and liquid do not generate important effects.

The inlet velocity (20 m/s) and the outlet pressure have been specified as boundary conditions. On both end-walls and hydrofoil surface no-slip conditions were imposed. For what concerns the turbulence scalar quantities, the inlet turbulence intensity is 5% and a turbulence length scale of 0.00375 m. This last value has been calculated considering 1/20 of the mid-height of the channel.

The analyses in cavitating conditions were conduced with a constant cavitation number σ of 0.81 and defined as reported in equation (1). The inlet pressure and velocity were selected as reference values.

$$\sigma = \frac{p_{ref} - p_{sat}}{\frac{1}{2}\rho_l U_{ref}^2} \tag{1}$$

Results

The pressure distributions along the profile are presented here in terms of pressure coefficient, defined as follows:

$$Cp = \frac{p - p_{ref}}{\frac{1}{2}\rho_l U_{ref}^2} \tag{2}$$

The reference values are the same defined above. Figure 2(a) shows the result obtained in non-cavitating conditions. A very good agreement can be observed between the experiments and the numerical data along all of the profile, except for the zone close to the trailing edge. Nevertheless, this misprediction can be accepted considering that the zone interested by the cavitating flow is well resolved. Figure 2(b) shows the pressure coefficients obtained with cavitating flow considering both cavitation models.

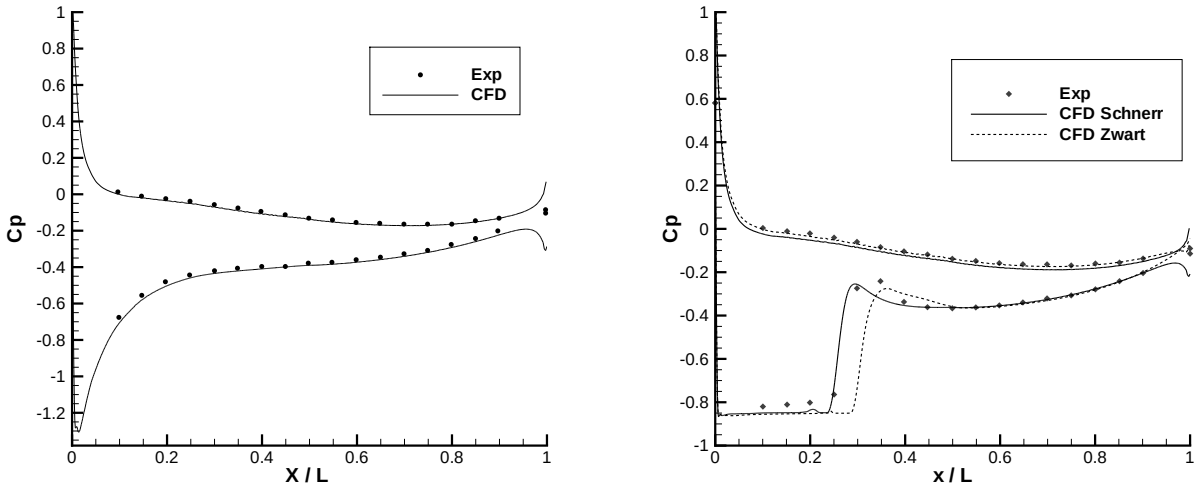

(a) (b)

Figure 2: **Pressure distribution on the profile in non-cavitating (a), and cavitating conditions with $\sigma = 0.81$ (b)**

On the pressure side of the profile both models provide a good agreement with experimental data and this is true also for the rear suction side. Both these zones are not noticeably influenced by cavitation. Solutions predicted with the two models differ in the portion of suction side included from the leading edge to 50% of the chord, where cavitation happens and the onset of the bubble influences the pressure distribution. Both models underestimate similarly the pressure coefficient up to 22% of the chord. The Schnerr-Sauer model well reproduces the pressure increase that the experiments show from 25% to 30% of the chord, while the Zwart-Gerber-Belamri model shows this pressure variation in the wrong position. The Schnerr-Sauer model also reproduces well the flow behavior after the cavitating zone while an overprediction of the flow acceleration can be observed at 27% of the chord. On the contrary, the pressure distribution given by the Zwart-Gerber-Belamri model does not reproduce the correct evolution of the cavitating zone and a larger volume of vapor is expected.

To better understand this behavior, Figures 3(a) and 3(b) show the vapor volume fraction contours obtained using the Schnerr-Sauer and Zwart-Gerber-Belamri models respectively. The second model predicts an extended cavitating zone with a bigger bubble with respect to the Schnerr-Sauer model. It is also interesting to observe how both models predict the typical re-entrant jet that occurs in the terminal zone of the attached bubbles.

Regarding the calculation stability, it can be said that both tested models had no convergence problem, but the Schnerr-Sauer model showed a faster convergence rate. According to the shown results, the Schnerr-Sauer cavitation model performs better than the Zwart-Gerber-Belamri and therefore it will be applied to a real pump geometry. Before doing this analysis, tests were performed with Schnerr-Sauer model by varying the bubble number density parameter. The aim of this investigation was to evaluate its influence on the prediction of cavitation. Values of 10^9, 10^{11}, 10^{13} and 10^{15} for the bubble number density were tested. The results show a substantial independence of the solution from this parameter except for the 10^9 case, as reported in Figure 4. Considering that in a range of four orders of magnitude no difference is visible, the simulations of a cavitating pump will be performed using the default value of 10^{13}.

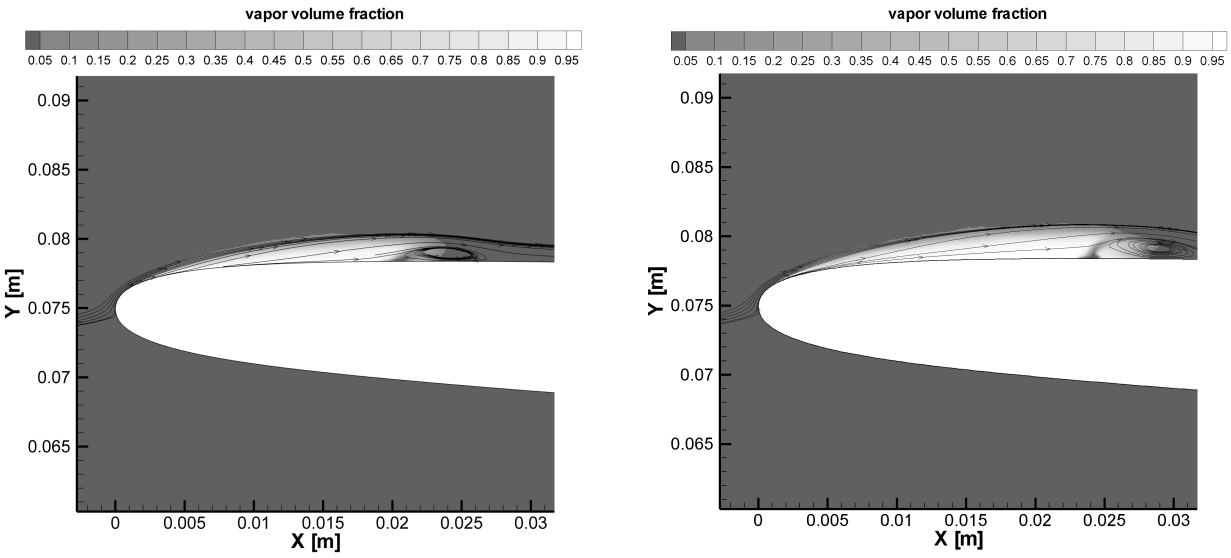

(a) (b)

Figure 3: **Contours of vapor volume fraction with superimposed streamlines in the front part of the profile, obtained with the Schnerr-Sauer model (a) and the Zwart-Gerber-Belamri model (b)**

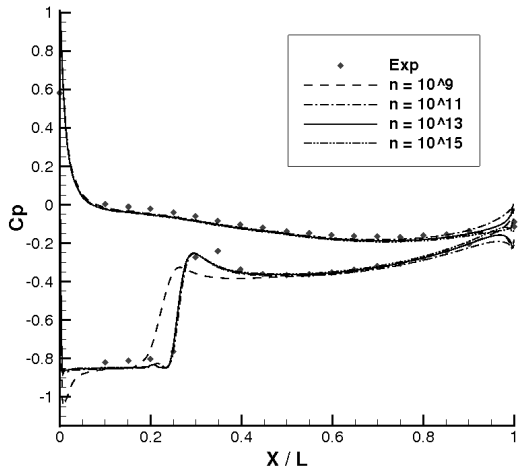

Figure 4: **Contours of pressure coefficient, obtained in cavitating conditions ($\sigma = 0.81$) with the Schnerr-Sauer model varying the bubble number density**

NUMERICAL ANALYSIS OF A CAVITATING IMPELLER

Description of the methodology

An in-line centrifugal pump produced by Weir Gabbioneta was investigated. The impeller has a specific speed of $N_s \simeq 1650$. An experimental campaign at full scale conditions was performed by Weir Gabbioneta. The experimental circuit can be schematized as reported in the Figure 5. The pump was characterized with H-Q and NPSHr-Q curves. The available experimental data for pressure measurements are referred only to the stations 0 and 6 (Figure 5). From a numerical point of

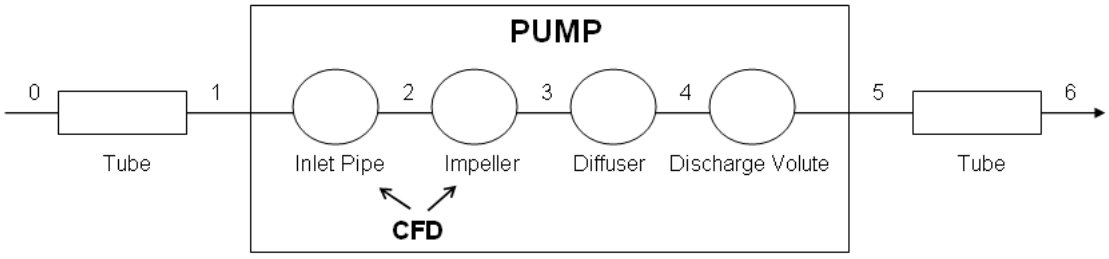

Figure 5: **Fluid network of the experimental set-up**

view, the pressure values must be evaluated in the same stations to compare the NPSHr. To reduce computational costs, only the inlet pipe and the impeller were simulated. This choice can be justified considering that the influence of the other components on the vapour formation in the impeller is negligible. 3D RANS single-phase simulations were performed for assessing the input data for the heuristic model. Hybrid unstructured grids were realized. The suction volute and the impeller grids contain about 320k and 1.85M elements respectively. A SST model was employed for the turbulence closure and the suction volute and the impeller were coupled through a "frozen rotor" approach. Starting from scratch a converged solution of the cavitating simulation has requested 120 hours on a Linux cluster with 4 processors and 8GB RAM.

Head was assessed by CFD simulations for the inlet pipe and the impeller, while the ones in the pump diffuser and in the ducts of the experimental set-up were esteemed by correlations. The characteristic of the flow field in a channel diffuser can be illustrated with the TEIS Model (Japikse *et al*. (1997)). This approach consists of dividing the object under investigation into two elements. For a channel diffuser the first element is the region between the impeller exit and the channel throat, the second element is the region between the throat and the channel exit. The first element is a highly complex, three dimensional, viscous and time dependent flow field (Japikse *et al*. (1997)). The pressure recovery in this region was evaluated through the correlation proposed by Kenny (1972). The boundary layer thickness in the diffuser throat is obtained by the correlation proposed by Kano *et al*. (1982). The pressure recovery in the second part of the diffuser was calculated applying the Bernoulli theorem under the hypothesis of steady state one-dimensional flow. Distributed head losses were assessed using the Moody formulation. The characteristic length was deduced by the geometry of the channel diffuser. At the diffuser outlet, the axial velocity component was supposed to be negligible, then the radial velocity was calculated for each flow rate knowing the area at the exit of the diffuser. The tangential component of the flow was evaluated considering that the exit flow angle is almost independent from the flow rate. Since the kinetic energy at the volute inlet is low, the pressure recovery in the discharge volute was neglected. Head drops in the tubes were evaluated applying the Bernoulli theorem while the Moody diagram was employed for the estimation of the distributed head losses. The concentrated head losses at the curves were evaluated as suggested by Idel'cik (1986).

Fixing the flow rate, the variation between the experimental and the numerical values of head is lower than 6% for all cases (Figure 6). Therefore, the proposed numerical procedure can predict in a satisfactory way the head referred to the whole experimental set-up.

Results of the two-phase simulations

The search for the NPSHr from two-phase simulations was performed following a procedure analogous to the experimental one. For each flow rate, starting from non cavitating conditions, the pressure at the pump inlet is reduced as long as the percent head drop respect to the non cavitating

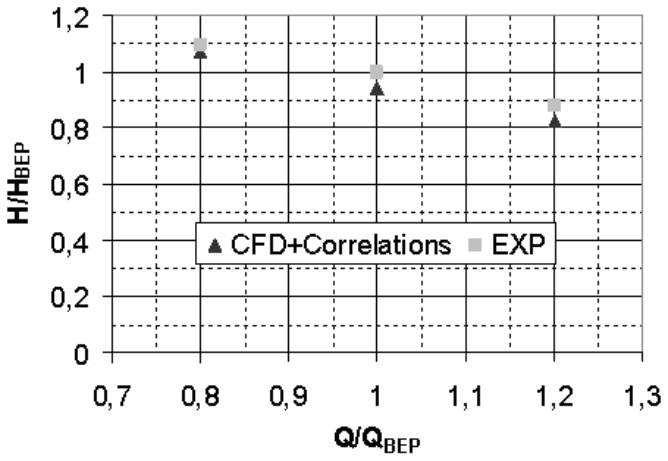

Figure 6: **Comparison between the experimental and numerical head**

Q/Q_{BEP}	$NPSHr_{CFD}/NPSHr_{BEP}$	$NPSHr_{EXP}/NPSHr_{BEP}$	$(NPSHr_{CFD}-NPSHr_{EXP})/NPSHr_{CFD}$ %
0,8	0,59	0,71	-16
1	0,79	1,00	-21
1,2	1,09	1,45	-24

Table 1: $\mathbf{NPSHr}_{CFD}$ **vs** $\mathbf{NPSHr}_{EXP}$

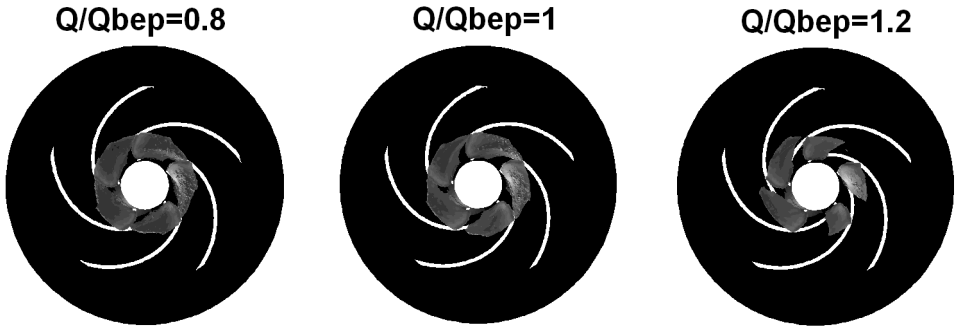

Figure 7: **Iso-surface of vapour volume fraction (at 99%) for the considered mass-flows**

values is equal to 3%. The head drop was calculated considering that vapour influences suction volute and impeller head only. For the other components of the fluid network (Figure 5) the correlations previously shown were adopted for the head esteem.

As reported in Table 1, the numerical analysis provides values of NPSHr which are much lower than the experimental one. Then, for each flow rate the inlet total pressure associated to the experimental NPSHr value is lower for the CFD simulations with respect to the experiments. The percent of pressure drop in the whole machine in cavitating conditions is strongly dependent by the amount of vapour produced. Considering the BEP flow rate in cavitating conditions, it can be said that an experimental test done considering the inlet total pressure given by the CFD will provide a higher amount of vapor production. Then, it can be concluded that the numerical analysis underestimates the steam production for each of the flow rates. The iso-surface of 99% of vapour volume fraction is reported in Figure 7 for each mass-flow evaluated. As can be seen, the volume of fluid interested by

cavitation decreases when the mass-flow increases.

A comparison between the CFD and the experimental local formation of vapour would be very helpful for justifying the different NPSHr prediction and for a further validation of the CFD procedure. Nowadays, experimental information about vapour production in the impeller are not available in the open literature. However, the proposed CFD methodology gives a NPSHr trend close to the experiments, with an error included between the 16% and 24%. The discrepancy between the experimental data and the numerical estimation is under investigation. It must be commented that the accuracy of the presented method is still too low to substitute, even partially, the experimental activity.

HEURISTIC MODEL

Problem formulation

This section details the outline of a preliminary study of a heuristic model for the definition of the NPSHr curve. The main idea of the study is to exploit classic monophase CFD simulations in order to relate the liquid pressure field with the quantity of cavitating flow. Namely, the objective is to define what portion of the flow is in cavitation conditions when the head falls to 3% with respect to nominal conditions. Once the model is validated, the knowledge of the portion of the fluid under the saturation pressure, will enable to evaluate the value of NPSH. The process is herein described.

The model has been assessed on two centrifugal pumps: the first is the above-mentioned in-line pump (IL), and the second one is a stage of the multi-stage centrifugal pump (AHPB), which has specific speed $N_s \simeq 2600$. Monophase calculations have been performed on the examined pumps at a reference pressure. Five different flow rates for IL and three for AHPB are considered. At these operating conditions the experimental values of NPSHr are available.

Two approaches have been used. The first approach is raised by the concept that the percentage of fluid volume which is subject to phase variation should be connected to the performance deterioration of the machine. The volume whose pressure is under the vapor saturation pressure is registered by its percentage to the total impeller volume. As a result, this fraction should therefore correspond to the volume of vapor arising in the impeller at 3% head drop conditions.

The other approach considers the percentage of blade surface where the flow pressure is lower than the saturation pressure. The procedure is similar to the one for volumes explained above, but this time the cell faces belonging to the blade surface are considered. Then the surface fraction which has pressure values under the saturation vapor pressure is considered as well. Afterwards, correlation between the percentage of cavitating surface and the flow rate are searched. The obtained coefficient is then scaled by a factor which is function of the ratio between current and *BEP* flow rate and the results are discussed in the following section.

Results

A post-processing code NPSearcH has been developed, whose inputs are the NPSHr value and inlet total pressure from the calculation, and the pressure values over the blades cell surface or impeller volume. Then the program outputs the value of blade surface or impeller volume percentage. The results of the procedure with volume approach are displayed in Figure 8.

These curves show that a linear relation exists between the volume percentage under cavitation conditions and volume flow rate, as at higher flow rates a lower fraction of vapor is sufficient for a 3% head drop. The post-processor has also been applied to the two-phase calculation (Figure 8), confirming the linear relation already observed for the monophase data. The linearly decreasing behavior of incipient cavitating fluid volume fraction with increasing volume flow rates can be explained considering that at higher flow rates the head decreases. It is therefore likely that the cavitating volume fraction leading to 3% head drop decreases. The IL pump can bear higher cavitating volume fraction before head falling down. Actually the NPSHr values for this machine are lower than about one third

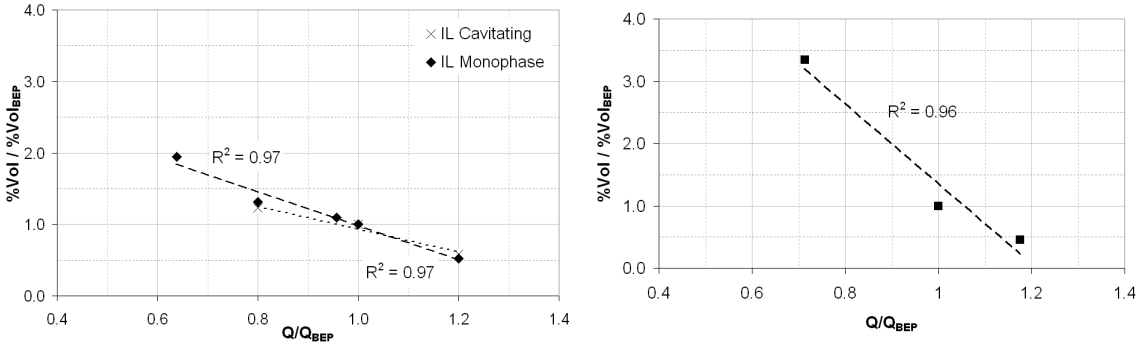

(a) (b)

Figure 8: **Percentage of impeller volume with pressure under vapor saturation pressure: IL (a), AHBP (b)**

of those for AHPB pump.

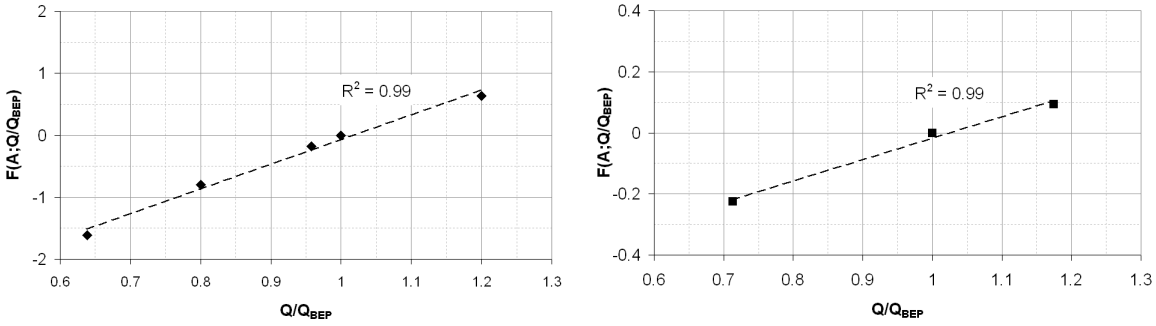

(a) (b)

Figure 9: **Percentage of cell faces on the blade surface with pressure under vapor saturation pressure: IL (a), AHBP (b)**

The curves resulting from the process with blade surface approach are shown in Figure 9. The tendency of these parameters is very well approximated by a linear curve for both pumps, with an increasing tendency with increasing flow rates. The knowledge of this curve for each machine allows then to verify how to use this correlation to define the NPSHr curve is accurate. Such definition of the parameter needs that the value of NPSHr at *BEP* is specified. Then, the NPSHr value for each different flow rate can be calculated by the knowledge of the surface fraction. The curves calculated with this method are displayed in Figure 10. The maximum error for IL pump is of 26%, while that for AHPB pump is 20%. For flow rates far from the *BEP* condition an accuracy of around 3% can be reached.

Performing more simulations with available experimental data on different centrifugal pumps is a further step which will enable us to conduct more detailed investigations on the linear behaviors which have been observed. This will allow investigating correlations which define the above-mentioned coefficients in relation to pump geometry and global performance parameters.

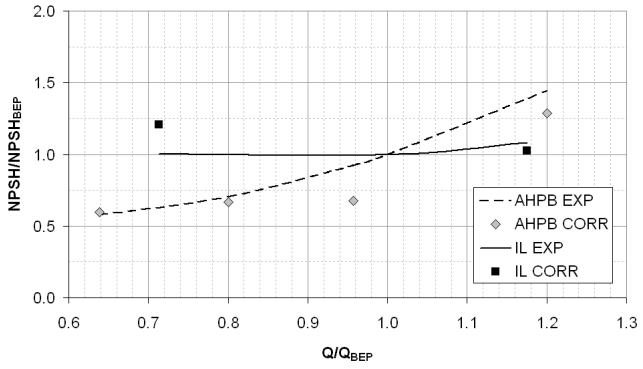

Figure 10: **NPSHr curve of IL and AHPB, experiments (line) and heuristic model (point)**

CONCLUSIONS

In this work numerical approaches for the evaluation of the cavitation in centrifugal pumps have been presented. Amongst the available cavitation models the approach proposed by Schnerr and Sauer (2001) was selected as the most accurate. The application of this model to an actual geometry allowed predicting the NPSHr of the pump with an error between 16% and 24% in the working range of the machine.

Furthermore, a correlation between the NPSHr and the cavitating volume has been presented and applied to monophase simulation of two pumps. By using this approach a linear function between the flow rate and the cavitating volume of fluid has been individuated. The trend is also confirmed by using the same approach on a two-phase simulation with cavitation. A similar result has been obtained when considering a combination between the fraction of cavitating blade surfaces and the flow rate. The application of this correlation provided the NPSHr curve for the two examined pumps with a precision up to 3%.

This is a promising approach for the evaluation of the NPSHr curve from a monophase simulation. Further calibration is necessary for the application to a wide range of geometries and working conditions during the design phase of brand new centrifugal pumps.

References

Brennen C.E., *Hydrodynamic of Pumps*, Concepts ETI, Inc. and Oxford University Press, 1994

Delannoy Y., Kueny J.L., *Two Phase Flow Approach in Unsteady Cavitation Modelling*, Cavitation and Multiphase Flow Forum, ASME-FED Volume 98, pp. 153-158, 1990

Dupont P., *Etude de la dynamique d'une poche de cavitation partielle en vue de la prediction de l'erosion dans les turbomachines hydrauliques*, PhD thesis, These No. 931, EPFL - Lausanne, 1991

Frobenius M., Schilling R., Bachert R., Stoffel B., Ludwig G., *Three-Dimensional Unsteady Cavitation Effects on a Single Hydrofoil and in a Radial Pump â Measurements and Numerical Simulations. Part Two: Numerical Simulation*, Proc. of the Fifth International Symposium on Cavitation, Osaka, Japan, November 1-4, 2003

Japikse D., Marscher W.D., Furst R.B., *Centrifugal Pump Design and Performance*, Concepts ETI, Inc., 1997

Kano F., Tazawa N., Fukao Y., *Study of Flow Distribution and Aerodynamic Performance of Centrifugal Compressor*, SAE Paper No. 820328, Turbocharger performance & application. SP-514, Society of Automotive Engineers, Inc., Warrendale, Pennsylvania, 1982

Kenny D.P., *A comparison of the predicted and measured performance of high pressure ratio centrifugal compressor diffusers*, Proc. of the ASME IGTI Conference, 72-GT-54, 1972 Wageningen, The Netherlands, 2006

Kunz F.K., Boger D.A., Stinebring D.R., Chyczewski T.S., Gibeling H.J., Venkateswaran S., Govindan T.R., *A Preconditioned Navier Stokes Method for Two-Phase Flows with Application to Cavitation Prediction*, AIAA-99-3329, 1999

Idel'cik I.E., *Memento des Pertes de Charge*, Eyrolles, Collection de la direction des Etudes et Recherches d'Electricite de France, 1986

Menter F.R., *Improved Two-Equation k-ω Turbulence Models for Aerodynamic Flows*, Technical Report, NASA Technical Memorandum 103975, 1992

Singhal A.K., Li H.Y., Athavale M.M., Jiang Y., *Mathematical Basis and Validation of the Full Cavitation Model*, ASME FEDSM 2001, New Orleans, Louisiana, USA, 2001

Schnerr G.H., Sauer J., *Physical and Numerical Modeling of Unsteady Cavitation Dynamics*, Proc. of 4th International Conference on Multiphase Flows, New Orleans, Louisiana, USA, 2001

Tamura Y., Matsumoto Y., *Improvement of Bubble Model for Cavitating Flow Simulations*, J. Hydrodynamics, Volume 21(1), pp. 41-46, 2009

Zwart P.J., Gerber A.G., Belamri T., *A Two-Phase Flow Model for Predicting Cavitation Dynamics*, Proc. of 5th International Conference on Multiphase Flows, Yokohama, Japan, 2004